

Observational test of the CH cation oscillator strengths

T. Weselak¹, G. A. Galazutdinov², F. A. Musaev³, Y. Beletsky⁴, and J. Kręłowski⁵

¹ Institute of Physics, Kazimierz Wielki University, Weysenhoffa 11, 85-072 Bydgoszcz, Poland
e-mail: towes@gazeta.pl

² Korea Astronomy and Space Science Institute, Optical Astronomy Division, 61-1, Hwaam-Dong, Yuseong-Gu, Daejeon, 305-348, Korea
e-mail: gala@kasi.re.kr

³ Special Astrophysical Observatory, Nizhnij Arkhyz, 369167, Russia
e-mail: faig@sao.ru

⁴ European Southern Observatory (ESO), Alonso de Cordova 3107, Santiago, Chile
e-mail: ybialets@eso.org

⁵ Center for Astronomy, Nicolaus Copernicus University, Gagarina 11, 87-100 Toruń, Poland
e-mail: jacek@astri.uni.torun.pl

Received 9 June 2008 / Accepted 21 November 2008

ABSTRACT

We revise measurements of the positions and oscillator strengths using spectral features in the CH⁺ *A* – *X* system, and by using high-resolution, echelle spectra of 36 stars and assuming that its wavelength and oscillator strength as given in the literature for the (0, 0) transition, i.e. 4232.548 Å and 0.00545 respectively, are correct. The recommended oscillator strengths of the lines at 3957.689, 3745.308, 3579.024, and 3447.077 Å are found to be (in units of 10⁻⁵) 342, 172, 75, and 40, respectively. The estimated column densities of the CH cation toward the observed targets are also presented.

Key words. ISM: molecules – ISM: abundances

Introduction

The CH⁺ radical plays a key role in gas-phase interstellar chemistry. It was one of the first molecules to be discovered in the interstellar medium (ISM) by Douglas & Herzberg (1941), together with CH and CN. Since then, its formation and existence in the ISM has remained an unsolved problem (van Dishoeck & Black 1996; Gredel 1993). However, the species appears to be ubiquitous, and we detect its presence by measurement of its high column densities toward a significant number of reddened OB stars.

The CH cation can be studied by detection of its optical absorption features, which are observed in the blue, violet, and near-ultraviolet from ground-based observatories. Its 4232 and 3957 Å lines, due to the (0, 0) and (1, 0) bands of the A¹Π – X¹Σ⁺ system, can be easily observed (Federman 1982; Gredel 1993; Weselak et al. 2008). Other lines of the *A* – *X* system at 3745 Å (2, 0), 3579 Å (3, 0) and 3475 Å (4, 0) were identified by Douglas & Morton (1960) and observed toward ζ Oph by Herbig (1968). However, these lines have not attracted the attention of observers.

Laboratory determinations (experimental and theoretical) of the oscillator strengths of transitions between the ground and first excited states are needed to determine the correct value of CH⁺ abundances toward observed targets. The oscillator strengths of the *A* – *X* (0, 0) at 4232 Å and *A* – *X* (1, 0) transition at 3957 Å are now well established by theoretical and laboratory experiments (see Larsson & Siegbahn 1983 as a review), whereas there is still a considerable spread in experimental and theoretical results concerning the *A* – *X* (2, 0), (3, 0), and (4, 0) transitions of the CH cation reported in the literature. It

should also be noted that the reported interstellar abundances of CH cation are directly related to the *A* – *X* oscillator strength.

We aim to complete measurement of the oscillator strengths of the observable *A* – *X* transitions of the CH⁺ molecule based on the observational intensities of aforementioned five transitions observable by ground-based telescopes. This should allow more precise measurement of the column densities of CH⁺ toward 36 reddened OB stars based on high-resolution, echelle spectra. We emphasize that while the most popularly observed CH⁺ bands can be saturated, the near-UV bands are not likely to be.

The observational data

Most of our observational material, listed in Table 1, was obtained using the UVES spectrograph at ESO Paranal in Chile with a resolution $R = 80\,000$. Our spectra cover the spectral range from 3040 to 10 400 Å¹.

The spectra of 5 objects were obtained with the HARPS spectrometer (labelled by superscript *H* in Table 1), mounted on the 3.6 m ESO telescope in Chile². This spectrograph allows us to cover the range ~3800–~6900 Å with a resolution of $R = 115\,000$. Since the instrument was designed to search for exoplanets, it is capable of providing data for precise wavelength measurements.

¹ They were acquired as part of the project “Library of High-Resolution Spectra of Stars across the Hertzsprung-Russell Diagram” and are available at the website: <http://www.sc.eso.org/santiago/uvespop>. For more information see Bagnulo et al. (2003).

² see <http://www.ls.eso.org/lasilla/sciops/3p6/harps/>

Table 1. Observational measurements and published data. Description is presented in the text.

Obs	HD	Spec/L	$E(B - V)$	W_{3447} [mÅ]	W_{3579} [mÅ]	W_{3745} [mÅ]	W_{3957} [mÅ]	W_{4232} [mÅ]	$N(\text{CH}^+)$ [10^{12} cm^{-2}]	W_{4232}^{Lit} [mÅ]	$N(\text{CH}^+)^{\text{Lit}}$ [10^{12} cm^{-2}]	S/N
58 343	B2Vne		0.14			1.70(0.34)	3.89(0.42)	6.87(0.67)	7.95 (0.78) ^a			400
68 761	B0.5III		0.14			2.10(0.31)	3.69(0.37)	5.78(0.60)	6.69 (0.69) ^a			390
76 341	B1/B2Ib		0.46	2.10(0.30)	3.86(0.45)	10.11(0.82)	22.66(1.23)	38.25(1.97)	47.35 (3.91) ^c			290
92 740	WN7		0.36			3.30(0.30)	6.79(0.71)	13.21(0.95)	15.29 (1.10) ^a			470
94 963	O6/O7IIIe		0.20			1.50(0.32)	3.86(0.43)	6.26(0.70)	7.25 (0.81) ^a			400
96 917	O8		0.37	1.20(0.30)		4.56(0.41)	8.57(0.93)	16.85(1.54)	19.50 (1.78) ^a			390
97 253	O5IIIe		0.50	1.46(0.35)		5.50(0.47)	10.63(0.86)	18.15(1.08)	21.01 (1.25) ^a			550
105 056	O9.5Ia		0.33			3.85(0.65)	10.37(1.12)	18.98(2.12)	21.97 (2.45) ^a			220
105 071	B6Ia/Iab		0.25			3.75(0.41)	6.57(0.53)	11.48(0.68)	13.29 (0.79) ^a			340
106 068	B8Ia/Iab		0.32	2.20(0.34)	3.79(0.40)	7.75(0.54)	16.9(0.61)	27.88(1.43)	35.65 (1.33) ^b			300
109 867	B0.5/B1Iab		0.26	0.90(0.30)		1.68(0.45)	5.51(0.54)	9.72(1.21)	11.25 (1.40) ^a			380
112 272	B1Ia/Iab		0.99			6.95(0.35)	16.26(0.86)	30.25(1.33)	35.01 (1.54) ^a			330
113 904	WC+O9.5		0.16			1.25(0.32)	2.92(0.35)	5.60(0.46)	6.48 (0.53) ^a	5.9(0.3) ^d	6.83(0.34) ^d	340
115 363	B1Ia		0.82			3.40(0.43)	8.63(0.87)	16.59(1.56)	19.20 (1.81) ^a			420
115 842	B0.5Ia		0.51			4.00(0.34)	9.79(0.94)	15.40(1.43)	17.82 (1.66) ^a			370
133 518	B2IVp...		0.09			1.72(0.41)	4.66(0.42)	9.60(1.08)	11.11 (1.25) ^a			330
142 758	B1Ia		0.41	1.40(0.34)		5.09(0.43)	10.03(0.93)	18.89(1.32)	21.86 (1.53) ^a			380
143 448	B2/B3III		0.11			1.35(0.29)	2.53(0.31)	4.76(0.61)	5.51 (0.71) ^a			420
^H 147 889	B2III/IV		1.02	3.10(0.45)		6.63(0.67)	15.93(0.93)	25.95(0.82)	33.60 (2.03) ^b	25.0(5.8) ^e	40.74(9.7) ^e	690
^H 148 184	B2Vne		0.43	1.25(0.31)		2.82(0.34)	6.33(0.43)	10.03(0.45)	11.61 (0.52) ^a	9.98(0.03) ^d	11.55(0.03) ^d	700
148 688	B1Ia		0.55	1.85(0.35)		6.10(0.56)	12.77(0.65)	23.21(0.84)	26.94 (1.42) ^a			480
148 937	O6e		0.67			3.27(0.42)	9.06(0.87)	17.63(1.24)	20.40 (1.44) ^a			360
151 932	WN7		0.50	1.21(0.32)		3.75(0.48)	7.22(0.65)	13.27(1.12)	15.36 (1.30) ^a			340
^H 152 235	B0.7Ia		0.73	1.85(0.32)	3.75(0.43)	11.22(0.66)	25.44(1.21)	42.29(1.62)	53.66 (2.64) ^b	42(5) ^f	58(-) ^f	650
152 270	WC7		0.50	1.00(0.30)	2.25(0.35)	5.31(0.43)	11.90(0.54)	22.90(0.93)	26.50 (1.08) ^a			310
154 368	O9Ia		0.80	1.00(0.30)	1.80(0.37)	4.15(0.35)	10.10(0.45)	17.20(0.89)	19.91 (1.03) ^a	17.5(0.4) ^d	20.25(0.46) ^d	510
154 811	O9.5Ib		0.66		2.96(0.43)	9.13(0.65)	19.03(1.23)	31.86(1.43)	41.48 (2.68) ^b			370
154 873	B1Ib		0.47		2.38(0.46)	5.35(0.34)	12.96(1.10)	21.06(0.85)	24.37 (0.98) ^a			350
155 806	O8Ve		0.32			2.78(0.31)	6.10(0.45)	9.05(0.67)	10.47 (0.78) ^a	8.0(0.2) ^d	9.26(0.23) ^d	320
156 385	WC7		0.34			2.87(0.36)	6.78(0.56)	13.07(0.76)	15.13 (0.88) ^a			440
156 575	B1Ib/II		0.40	2.80(0.37)		5.61(0.42)	11.48(0.87)	23.96(0.93)	27.73 (1.08) ^a			360
^H 163 800	O7/O8		0.58	0.50(0.07)	1.25(0.32)	3.97(0.43)	7.69(0.41)	13.42(0.43)	15.53 (0.50) ^a			420
164 794	O4V...		0.36			2.34(0.31)	4.67(0.34)	9.32(0.54)	10.79 (0.62) ^a			350
170 235	B2Vnne		0.29			1.39(0.29)	3.16(0.32)	6.51(0.45)	7.53 (0.52) ^a			400
171 432	B1/B2Iab		0.43			2.25(0.34)	7.30(0.53)	11.97(0.56)	13.85 (0.65) ^a			430
^H 179 406	B3V		0.31				1.67(0.40)	3.60(0.50)	4.17 (0.60) ^a			500

All the spectroscopic data were reduced with standard packages of MIDAS and IRAF, as well as our own DECH code (Galazutdinov 1992), which provides all the standard procedures of image and spectra processing. Using different algorithms to complete the data reduction reduces the possibility of inaccuracies due to use of slightly different approaches to dark subtraction, flatfielding, or removal of cosmic ray hits. Most of our spectra from UVES were also taken from the archive as pipeline-reduced products³, which allowed another comparison of the precision of the measured wavelengths.

For this project, we selected a sample of 36 reddened stars for which the CH cation bands at 3745, 3957, and 4232 Å were seen. Most of our objects were acquired using the UVES spectrograph but some were from HARPS, which is capable of higher wavelength precision. For objects observed with the HARPS instrument, the error in the wavelength measurement did not exceed the value of 0.001 Å (in general radial-velocity accuracy is not higher than 30 m/s – see HARPS user manual).

Table 1⁴ presents the HD numbers, spectral types, luminosity classes, and the $E(B - V)$ of each star, and the equivalent widths (W_{λ} s) (in mÅ) of CH⁺ bands at 3447, 3579, 3745, 3957, and 4232 Å. We also present column densities calculated for unsaturated CH⁺ bands. To measure the column density, we used the relation of van Dishoeck & Black (1989), which provides proper column densities when the observed lines are unsaturated:

$$N = 1.13 \times 10^{20} W_{\lambda} / (\lambda^2 f), \quad (1)$$

where W_{λ} and λ are in Å and column density in cm⁻². To measure the column density, we adopted the f -value of

⁴ In Table 1 we present HD number, spectral type, and luminosity class, $E(B - V)$, equivalent widths (EW s) (in mÅ) of CH⁺ bands at 3447, 3579, 3745, 3957 and 4232 Å. We also present column density calculated on the basis of unsaturated CH⁺ bands at a – 4232, b – 3957, and c – 3745 Å depending on whether the 4232 and 3957 bands are saturated or not. For the 3957 Å band, we adopted a new f -value equal to 342×10^{-5} . We also compare our column densities with those presented in the literature (d – Weselak et al. 2008; e – Allen 1994; f – Crawford 1989). In the last column, the calculated signal-to-noise ratio in the vicinity of 4232 Å band (after normalization) is presented.

³ See UV-Visual Echelle Spectrograph user manual at <http://www.eso.org/sci/facilities/paranal/>

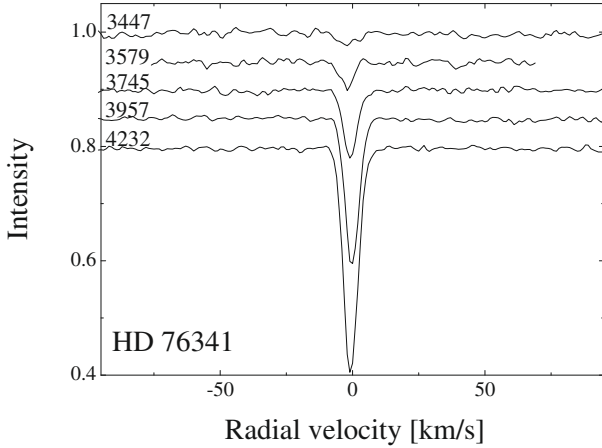


Fig. 1. The (0, 0) to (0, 4) systems of CH cation $A - X$ transitions, presented in the spectrum of HD 76 341 on a radial-velocity scale.

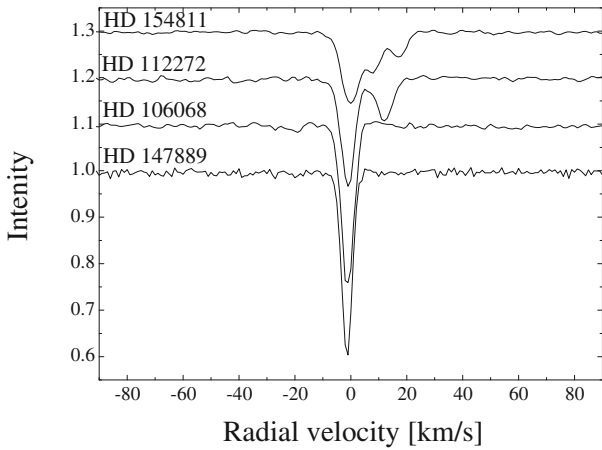


Fig. 2. Spectral features of CH^+ $A - X$ band at 4232 Å shown in the radial-velocity scale. The saturation effects are easily seen in the case of HD 106 068 and 147 889.

Larsson & Siegbahn (1983) for the CH^+ $A - X$ (0,0) transition and the new f -values obtained in this paper in the case of the CH^+ $A - X$ (1, 0), and (2, 0) transitions. The latter were used when $A - X$ (0, 0) and/or (1, 0) bands at 4232, and 3957 Å were saturated (HD's 76 341, 106 068, 147 889, 152 235, and 154 811). In the last three columns, we compare our results with those published previously and present the signal-to-noise ratio of each spectrum calculated close to the 4232 Å feature of CH^+ (equivalent widths of this band are given in mÅ, and the total column density of CH cation in cm^{-2} .)

Results and discussion

Figure 1 presents (on a radial-velocity scale) all the aforementioned spectral features of CH^+ observed in the spectrum of HD 76 341. In this case both 3957 Å and 4232 Å features are saturated since $W_\lambda > 20$ mÅ (see Table 1) and no Doppler-splitting can be traced in our high-resolution spectra.

In Fig. 2, the $R(0)$ line of (0,0) CH^+ $A - X$ transition is presented in the spectra of four stars. In the case of HD 112 272, the 4232 Å band is split into two components. The profile of the band in HD 154 811 splits into 3 components. The effects of saturation are easily seen only in the cases of HD 106 068

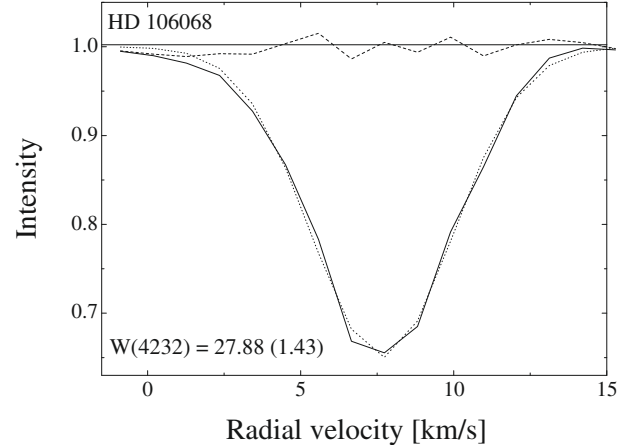
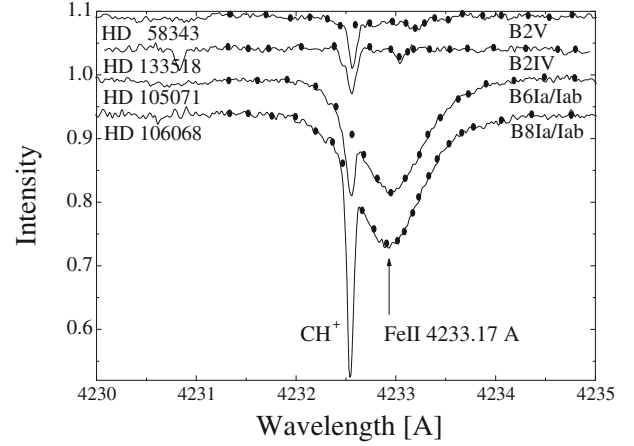


Fig. 3. Spectra of HD 58 343, 133 518, 105 071, 106 068 in the region of 4232 Å contaminated with the stellar feature of FeII at 4232.17 Å. We indicate correct continuum placement in each case (*at the top*). Below we present the measurement of equivalent width of the 4232 Å line in the spectrum of HD 106 068. Gaussian fits are marked with dots and residual intensity with dashed line. Note that the spectrum was not shifted along the radial-velocity scale during equivalent-width measurement.

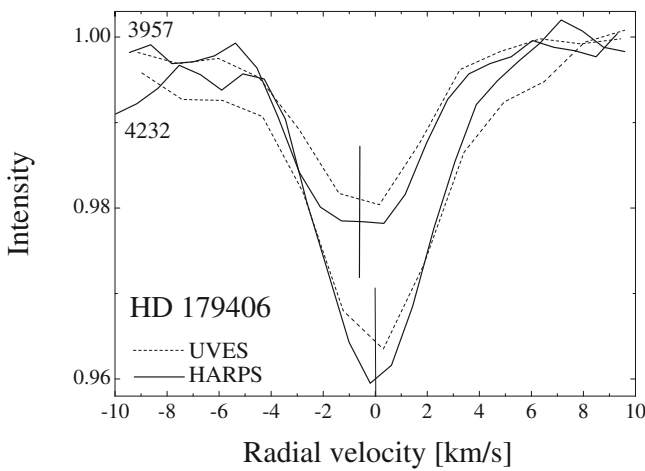
and 147 889, where one Doppler component is seen with $W_\lambda > 20$ mÅ (see Table 1). However, our spectra not of sufficiently high resolution to measure directly the Doppler broadening parameter. Therefore it is impossible to perform the test for the Doppler parameter determination directly from the apparent line width after correction for the finite resolution of the spectrograph.

Correct continuum placement is a serious problem for spectra contaminated with stellar lines. In Fig. 3, we present spectra of four objects of stellar type B2 and later, spectra in which the stellar FeII line at 4233.17 Å is present. After the continuum placement, we fitted a Gaussian function to each spectral line to derive its equivalent width. This is evident in the spectrum of HD 106 068, where FeII stellar line was blended with the CH^+ band at 4232 Å. It must be emphasized that correctness of the continuum placement is the main factor in determining the size of errors during equivalent width measurement. In the case of each spectral line, the procedure presented in Fig. 3 was performed. The error estimates were completed using the formulation of Smith et al. (1984). The errors determined for each fit are presented in Table 1.

It was also possible to improve line positions due to the fact that our spectra from HARPS and UVES instruments are

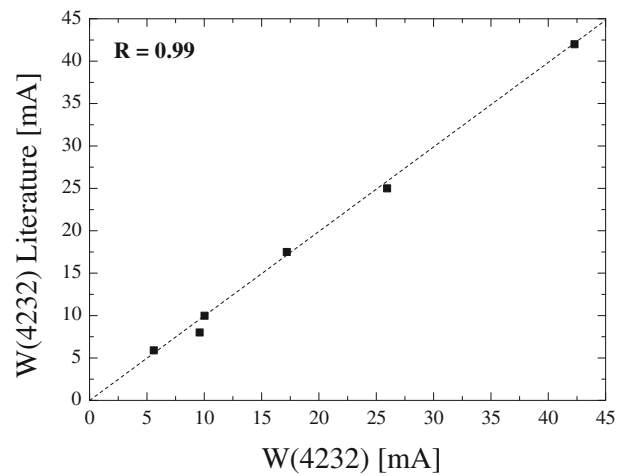
Table 2. New positions of CH⁺ molecular features compared to those of Herbig (1968) and Carrington & Ramsay (1982).

HD	Obs	4232 [Å]	3957 [Å]	3745 [Å]	3579 [Å]	3447 [Å]
76 341	<i>u</i>	4232.548	3957.688	3745.310	3579.029	3447.074
106 068	<i>u</i>	4232.548	3957.682	3745.308	3579.017	3447.078
147 889	<i>h</i>	4232.548	3957.688			
	<i>u</i>	4232.548	3957.687			
163 800	<i>h</i>	4232.548	3957.691			
	<i>u</i>	4232.548	3957.691	3745.305	3579.026	3447.079
179 406	<i>h</i>	4232.548	3957.691			
	<i>u</i>	4232.548	3957.693			
This work position		4232.548	3957.689	3745.308	3579.024	3447.077
Error			0.003	0.002	0.006	0.003
Herbig (1968)		4232.539	3957.700	3745.310	3579.020	3447.070
Carrington & Ramsay (1982)		4232.548	3957.692			

**Fig. 4.** Radial-velocity shift between 4232 and 3957 Å CH⁺ bands in the spectrum of HD 179406. Observed difference is equal to 0.580 ± 0.005 km s⁻¹. The effect is clearly seen by two different instruments, i.e. two independent instruments confirm this result.

of high resolution. However, after shifting the wavelength scale to ensure correct positions of CH at 4300.313 Å and CaI at 4226.728 Å, the differences in the wavelength scale between CH⁺ A – X bands at 4232 and 3957 Å remain. In Fig. 4 we present a shift in the radial-velocity scale between (0,0) and (1,0) A – X bands of CH cation observed in the spectra of HD 179406, acquired with two different instruments. The observed shift in our spectra does not have an instrumental origin and equals 0.580 ± 0.005 km s⁻¹ with a standard deviation inferred from the radial-velocity measurement in each case (the respective standard-deviation errors measured for the 4232 Å and 3957 Å lines were 0.10 and 0.10 km s⁻¹, and 0.10 and 0.09 km s⁻¹ for spectra from the UVES and HARPS instruments, respectively). This value clearly exceeds the precision of the wavelength determination of the HARPS spectrograph and thus at least one of the well-known wavelengths must be determined incorrectly.

Based on our high-resolution spectra of objects, in which no Doppler splitting of molecular features was observed, it was possible to obtain positions of CH⁺ A – X bands. In each case, we used the wavelength of CH⁺ A – X band at 4232.548 Å (Gredel et al. 1989) as the standard, i.e. we assumed its literature value to be correct. The results are presented in Table 2, which compares our values with those published previously by Herbig (1968)

**Fig. 5.** Our $W(4232)$ measurements are compared to those published in the literature. The relation is good with the correlation coefficient equal to 0.99.

and Carrington & Ramsay (1982). The observed differences do not exceed 0.010 Å. However, they exist for our high-resolution spectra from HARPS and UVES spectrographs.

Our measurements of equivalent widths were also compared with those published previously in the literature. As seen in Fig. 5, our measurements are closely related ($r = 0.99$) to those already published by Crawford (1989), Allen (1994), and Weselak et al. (2008). Column densities do not differ from those already published – given in the last column of Table 1. Only in the case of HD 147 889 is the difference evident, probably due to saturation effects that were not properly taken into account by Allen (1994).

The intensity ratio of two unsaturated spectral lines equals to:

$$\frac{W_{\lambda_1}}{W_{\lambda_2}} = \frac{f_1 \lambda_1^2}{f_2 \lambda_2^2} = \frac{q_1 \lambda_1}{q_2 \lambda_2} \quad (2)$$

where W_{λ_1} , W_{λ_2} are equivalent widths; f_1 , f_2 oscillator strengths (f -values), q_1 , q_2 Franck-Condon (F-C) factors, and λ_1 , λ_2 are the wavelengths of the lines under consideration. Equation (2) describes the ratio of the equivalent widths of two different lines of the same molecule in relation to their wavelengths and the Franck-Condon factors, and holds true if and only if (a) the lines arise in the same lower state, (b) the lines are the same branch in

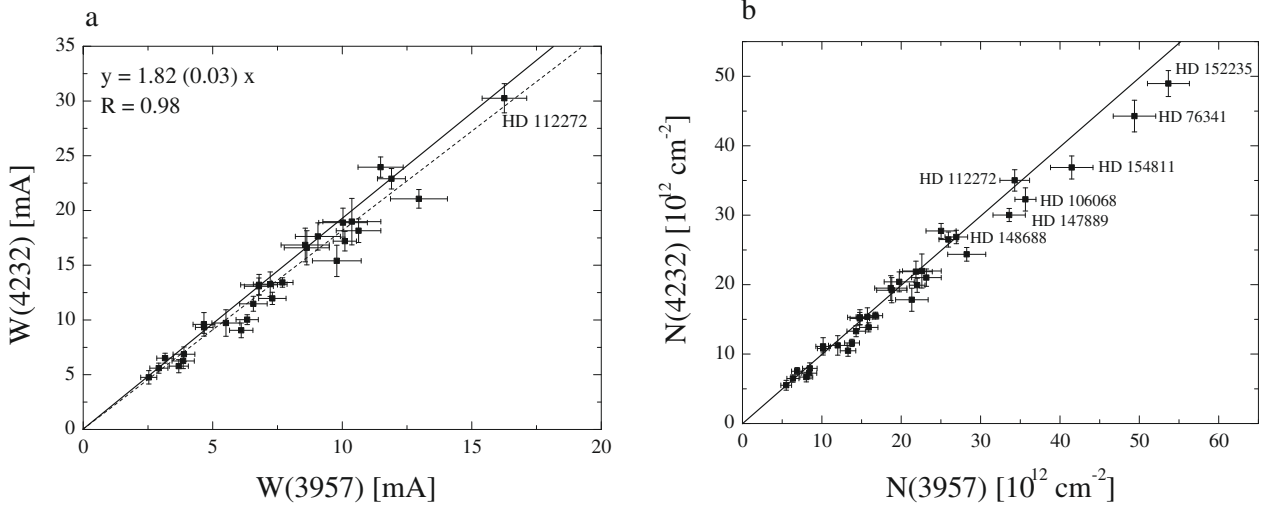


Fig. 6. The relation between equivalent widths of 3957 and 4232 bands **a)** and relation between their calculated column densities **b)**. In the case of equivalent widths, the solid line represents the W_λ 's ratio calculated in the absence of saturation using the oscillator strengths of Larsson & Siegbahn (1983). The dotted line is the fit to the data-points. In the case of column densities, the solid line represents equal values derived from both bands. In Fig. 6b, the Doppler splitting seen in HD 112 272 and 148 688 extends the range of the unsaturated part of the curve of growth.

Table 3. Calculated observed W_λ ratios with errors.

λ	4232	3957	3745	3579
4232				
3957	1.82 ± 0.03			
3745	4.04 ± 0.11	2.21 ± 0.04		
3579	9.99 ± 0.53	5.64 ± 0.26	2.75 ± 0.13	
3447	21.37 ± 2.49	11.23 ± 0.10	4.96 ± 0.50	1.89 ± 0.08

both bands, and (c) the dipole moment function is constant. (For more information see Larsson (1983).)

The calculated W_λ 's ratio of the 4232 Å and 3957 Å bands should equal 1.88 (where the f -values are equal to 545 and 331×10^{-5} , respectively Larsson & Siegbahn 1983) when both features are not saturated. The fit to our data-points is close to this value (1.82 ± 0.03) as seen in Fig. 6a. The relation between calculated column densities obtained using W_λ 's of 3957 Å and 4232 Å bands of CH cation is also seen in Fig. 6b. The Doppler splitting, probably observable in interstellar features, can extend the range of W_λ 's for which the saturation is not observed. We emphasize that the straight line representing the column densities, was fitted in the absence of saturation. Data points indicated by crosses are for HD 112 272 (the object with evident Doppler splitting). In general, the column densities of CH⁺, calculated from unsaturated 4232 Å and 3957 Å features coincide reasonably well.

In Fig. 6a, it can be well seen, that the line representing the ratio of equivalent width measurements for the 4232 and 3957 Å features, does not precisely fit the data-points. If we use the value of 545×10^{-5} in the case of CH⁺ A – X (0, 0) transition, then the f -value of (1, 0) transition should equal $342 \pm 6 \times 10^{-5}$. When the latter value is adapted, one can obtain f -values equal to 172 ± 9 for (2, 0), 75 ± 8 for (3, 0), and $40 \pm 5 \times 10^{-5}$ in the case of (4, 0) transition. In Table 3, we present calculated equivalent-width ratios for each CH⁺ A – X band with errors.

In Table 4⁵, we present the calculated oscillator strengths for all CH cation A – X transitions and F-C ratios, and compare them with the results presented in literature. In the fifth column of Table 4, we present how f -values of CH cation A – X transitions varied in the past. It is evident that theoretical and experimental f -values differ from publication to publication. Our results are based on the f -value that equals 545×10^{-5} in the case of CH⁺ A – X (0, 0) transition at 4232 Å presented by Larsson & Siegbahn (1983). Our new f -value in the case of (1, 0) transition at 3957 Å is higher than that presented in Larsson & Siegbahn (1983). Our f -value for the CH⁺ A – X (2, 0) transition at 3745 Å (172×10^{-5}) is close to that published previously by Elander et al. (1977) and Yoshimine et al. (1973) (170 and 173×10^{-5} , respectively). The f -value of the CH⁺ A – X (3, 0) transition at 3579 Å (75×10^{-5}) is higher than that published by Elander et al. (1977), which equals 63×10^{-5} ; based on theoretical calculations. However, it is difficult to compare our results with those published previously since no errors in the case of f -values of (1, 0), (2, 0), and (3, 0) A – X transition of CH⁺ molecule were estimated in the previously published theoretical works. It is also impossible to compare our result concerning (4, 0) with literature values because no data concerning f -value of this transition has been published.

In Table 4, we also compare the $f(v', 0)/f(0, 0)$ ratio with that based on data of Herbig (1968) and Frisch (1972). Our values differ from those published previously. We emphasize that our results are based on a new statistically meaningful sample of high-resolution spectra. We also compared the ratio of F-C factors $q(v', 0)/q(0, 0)$ with that following the data published by Herbig (1968) which was based on the Morse potential. It is well seen in the last column of Table 4 that our F-C ratios are close

⁵ In Table 4 we present the calculated oscillator strengths for all CH cation A – X transitions (v', v'') based on the f -value of Larsson & Siegbahn (1983) – (L83) for the 4232 band; other f -values follow our observations as well the calculated $f(v', 0)/f(0, 0)$ ratio and Franck-Condon factors $q(v', 0)/q(0, 0)$ ratio. Our results are compared with those already published: E77 – Elander et al. (1977), F72 – Frisch (1972), H68 – Herbig (1968), M(81) – Mahan & O'Keefe (1981), Y73 – Yoshimine et al. (1973).

Table 4. Calculated oscillator strengths for all CH cation $A - X$ transitions. Description is presented in the text.

$(v', v'') \lambda$	f [10^{-5}]	$f(v', 0)/f(0, 0)$	$q(v', 0)/q(0, 0)$	f^{Lit} [10^{-5}]	$f(v', 0)/f(0, 0)^{\text{Lit}}$	$q(v', 0)/q(0, 0)^{\text{H68}}$
(0, 0) 4232	545 ^{L83}	1	1	545 ^{L83} , 566 ± 20 ^{M81} , 645 ^{Y73} , 743 ^{E77}	1.000 ^{H68}	1.000
(1, 0) 3957	342 ± 6	0.628 ± 0.010	0.587 ± 0.009	331 ^{L83} , 431 ^{Y73} , 426 ^{E77}	0.555 ^{H68} , 0.548 ^{F72}	0.533
(2, 0) 3745	172 ± 9	0.316 ± 0.017	0.279 ± 0.008	173 ^{Y73} , 170 ^{E77}	0.335 ^{H68}	0.197
(3, 0) 3579	75 ± 8	0.138 ± 0.008	0.116 ± 0.006	63 ^{E77}	0.189 ^{H68}	0.068
(4, 0) 3447	40 ± 5	0.073 ± 0.003	0.0059 ± 0.0010	–	0.082 ^{H68}	0.026

to those previously published by Herbig (1968), in the case of (1, 0) and (2, 0) transitions.

Conclusions

The above considerations led us to infer the following conclusions:

1. our statistically meaningful sample of high resolution, high S/N ratio spectra allowed us to make more precise estimates of the oscillator strengths of $\text{CH}^+ A - X$ transitions, except in the case of $A - X (0, 0)$ for which we adapted the f -value proposed by Larsson & Siegbahn (1983);
2. comparing the radial-velocity scale of the 4232 Å and 3957 Å bands in the spectra of 5 stars (Table 2) allowed us to propose a new rest wavelength for the (2, 0) transition, which should be 3957.689 Å.

It is important to collect precise f -values from observational material and compare them to experimental and theoretical results. More efforts should be made for known visible transitions of diatomic molecules. It is certainly important to collect more spectra of sufficiently high signal-to-noise ratio to obtain correct f -values in the case of observable transitions. This procedure should allow us to adjust the column densities of all known molecules toward observed targets.

Acknowledgements. The authors acknowledge the financial support: J.K. and T.W. acknowledges that of the Polish State during the period 2007–2010 (grant N203 012 32/1550). We are grateful to anonymous referee for valuable suggestions that allowed us to improve the manuscript.

References

- Allen, M. 1994, ApJ, 424, 754
 Bagnulo, S., Jehin, E., Ledoux, C., et al. 2003, Msng, 114, 10
 Carrington, A., & Ramsay, D. A. 1982, Phys. Scr., 25, 272
 Crawford, I. A. 1989, MNRAS, 241, 575
 Douglas, A. E., & Herzberg, G. 1941, ApJ, 94, 381
 Douglas, A. E., & Morton, J. R. 1960, ApJ, 131, 1
 Elander, N., Oddershede, J., & Beebe, N. H. F. 1977, ApJ, 216, 165
 Federman, S. R. 1982, ApJ, 257, 125
 Frisch, P. 1972, ApJ, 173, 301
 Galazutdinov, G. A. 1992, Prep. Spets. Astrof. Obs., 92
 Gredel, R., van Dishoeck, E. F., & Black, J. H. 1993, A&A, 269, 477
 Herbig, G. H. 1968, ZA, 68, 243
 Larsson, M. 1983, A&A, 128, 291
 Larsson, M., & Siegbahn, P. E. M. 1983, Chem. Phys., 76, 175
 Mahan, B. H., & O'Keefe, A. 1981, ApJ, 248, 1209
 Smith, W. H., Schempp, W. V., & Federman, S. R. 1984, ApJ, 277, 196
 van Dishoeck, E. F., & Black, J. H. 1989, ApJ, 340, 273
 Yoshimine, M., Green, S., & Thaddeus, P. 1973, ApJ, 196, 307
 Weselak, T., Galazutdinov, G. A., Musaev, F. A., & Krelowski, J. 2008, A&A, 479, 149